

# Regulation of metal content and porous structure for Co-ZIF derived oxygen reduction reaction catalyst

Haoyang Zhao, Xintian Li, Weikang Zhu, Junfeng Zhang\*, Yan Yin\*

State Key Laboratory of Engines, Tianjin University

## ABSTRACT

Compared with Pt/C catalysts, non-precious metal (NPM) catalysts, with the advantages of low price and high natural abundance, have received extensive attention as the competitive candidate for fuel cell cathode oxygen reduction reaction (ORR) catalyst. Due to the low metal content and active site density of traditional NPM catalysts, higher catalyst loading is commonly required in real fuel cell applications. However, the thicker catalyst layer will lead to the high mass transfer resistance, reducing the performance of NPM catalyst layer, especially in high current density region. This study provide a new idea for high Co-content catalyst design, based on the SiO<sub>2</sub> coated zeolite imidazole framework (ZIF) material. By adjusting the Zn/Co ratio in the ZIF precursor and with or without the protection of and by exploring the influence of coated on the change of SiO<sub>2</sub>, the ZIF microstructure and Co nanoparticle size were carefully optimized. The introduction of SiO<sub>2</sub> shell can effectively avoid the agglomeration of metal nanoparticles, during the high-temperature activation process. However, protective effect of SiO<sub>2</sub> is also significantly different for ZIF precursors with different Zn/Co ratios. When the Co content in the catalyst precursor is higher (15%), SiO<sub>2</sub> shell can significantly reduce the metal nanoparticle size, which provide a new insight for high metal content catalyst design of alkaline fuel cell cathode catalyst.

**Keywords:** non-precious metal, Co-N-C catalyst, SiO<sub>2</sub>, Oxygen reduction reaction

## 1. INTRODUCTION

The oxygen reduction reaction (ORR) process in the cathode is one of the essential electrochemical process for polymer electrolyte membrane fuel cell performance.

Selection and peer-review under responsibility of the scientific committee of the 13<sup>th</sup> Int. Conf. on Applied Energy (ICAE2021).

Copyright © 2021 ICAE

At present, Pt-based precious group metal (PGM) catalysts are still the mainstream catalyst for fuel cell application due to its high electrocatalytic activity, but the low natural abundance and high price hinder its further commercialization. Co-N-C catalysts have been widely studied to replace commercial Pt/C catalysts due to their cost-effectiveness and high natural abundance.[1] To improve the activity and stability of non-precious metal (NPM) catalysts, the high-temperature activation process was used to form robust active site for oxygen reduction reaction (ORR). However, the pyrolysis process will irreversibly lead to the agglomeration of metal nanoparticles of NPM based catalyst, due to the high surface energy of metal nanoparticles. To avoid the formation of large metal particles as much as possible, researchers have developed abundant method to obtain NPM catalyst with highly dispersed active sites, such as coordination, defect engineering and spatial confinement. Among them, Zn-based zeolite imidazole framework (ZIF-8) with abundant micropores and nitrogen was always used as the precursor for highly dispersed NPM-based catalyst. As the pore forming agent, the content of Zn will directly determine the pore structure and active site density. Excess Zn will lead to the atomic dispersed active with very low active density. Although, the high kinetic activity of atomic dispersed catalyst can be obtained by rotating disk electrode (RDE), the very thick catalyst layer in the fuel cell is not conducive to the mass transfer process of gas and liquid, leading to the rapid decay in high current density region. [2] Coating a SiO<sub>2</sub> shell on the catalyst surface is a widely used strategy to prevent metal agglomeration under high-temperature activation. [3] This may provide a strategy to fabricate the NPM catalyst with high metal content and relatively smaller particle size. However, there is few research work focusing on the interactive relationship between SiO<sub>2</sub> shell and active

metal content during catalyst fabrication and the influence of its catalytic activity.

In previous studies, only one kind of metal content catalyst was studied, indicating that silica protection can prevent metal nanoparticles from agglomerating. In this study, SiO<sub>2</sub> protection strategy was introduced into different Co content ZIF precursor to explore the influence to the Co metal particles and catalytic activity of the final Co-based ORR catalyst. It was found that SiO<sub>2</sub> coating can effectively inhibit the agglomeration of Co element. Compared with previous ZIF-derived catalyst, the Co content can be increased obviously, benefiting from the protection of SiO<sub>2</sub> shell. The research results are expected to provide certain theoretical guidance for the high metal content NPM catalyst design to improve the catalytic and mass-transfer performance in following fuel cell application.

## 2. EXPERIMENTAL

### 2.1 Synthesis of Zn<sub>x</sub>Co<sub>1-x</sub>-ZIF Precursor

Typically, metal ions (total 10.8mmol) are composed of Zn<sup>2+</sup> (9.18mmol, 85%) and Co<sup>2+</sup> (1.62mmol, 15%), deriving from anhydrous zinc acetate (1.684g) and cobalt nitrate hexahydrate (0.4715g), respectively. These metal salts were dissolved in 200 mL of methanol and ultrasonicated for 5 minutes to obtain a uniform solution. In addition, 4.43g (54 mmol) of 2-methylimidazole (2-MI) was dissolved in 160 mL of methanol by ultrasonic treatment to obtain a uniform solution. The above two methanol solutions were mixed at ice-water temperature under magnetic stirring (800 rpm) for 40 min, and then allowed to stand at room temperature for 24 h (without stirring) to obtain a Zn<sub>0.85</sub>Co<sub>0.15</sub>-ZIF precursor. Under the premise of the same total amount of metal, different Zn<sub>x</sub>Co<sub>1-x</sub>-ZIF (x=0.85, 0.90) precursors were synthesized by increasing the ratio of Zn from 0.85 to 0.90 and reducing the ratio of Co from 0.15 to 0.10.

### 2.2 Synthesis of Zn<sub>x</sub>Co<sub>1-x</sub>-ZIF@SiO<sub>2</sub> Precursor

Zn<sub>x</sub>Co<sub>1-x</sub>-ZIF (200 mg) was dispersed in 60 mL ethanol, 4 g 2-methylimidazole was dissolved in 64 mL ultrapure water, the two solutions were mixed and 4 mL cetyltrimethyl ammonium bromide (CTAB) was added (25 mg mL<sup>-1</sup>). Then, 240 μL of tetraethyl orthosilicate (TEOS) was added dropwise. After magnetic stirring for 1.5 h under 800 rpm, the ZIF-SiO<sub>2</sub> particles were collected by centrifugation and washed with ethanol for three times. Dry at 60 °C for 12 h in a vacuum to obtain the final Zn<sub>x</sub>Co<sub>1-x</sub>-ZIF@SiO<sub>2</sub> precursor.

### 2.3 Fabrication of 1-xCo-N-C Catalysts

All the precursors were subjected to the same pyrolysis process to directly obtain the final catalyst without any post-treatment. Pyrolysis was carried out in a tube furnace at 950 °C for 2 hours under the protection of Ar atmosphere (200 mL min<sup>-1</sup>). After that, the samples were left under a continuous flow of inert gas overnight until they reached room temperature. The catalysts derived from different precursors with different Co content (Zn<sub>x</sub>Co<sub>1-x</sub>-ZIF, x=0.85, 0.9) are denoted as 1-xCo-N-C (x=0.15, 0.10), respectively.

### 2.4 Fabrication of 1-xCoSi-N-C Catalysts

The pyrolysis step is the same as the process described in 2.3. After pyrolysis, the SiO<sub>2</sub> shell needs to be etched in 40 mL of sodium hydroxide solution (5 mol L<sup>-1</sup>), stirred overnight at 45°C. The final catalyst powder was obtained by centrifugal separation, water washing and vacuum drying. Catalysts with different Co content are represented as 1-xCoSi-N-C (X=0.85, 0.90)

### 2.5 Characterization

Field-emission transmission electron microscope (FE-TEM) images were obtained on a JEM-2100F FE-TEM (JEOL) instrument. X-ray diffraction (XRD) patterns of the catalysts were obtained on a diffractometer (D8-Focus) using the Cu Kα radiation (k = 0.15418). X-ray photoelectron spectral (XPS) patterns were recorded using an X-ray photoelectron spectrometer (Thermo ESCALAB 250XI) with an aluminum (mono) Kα source (1486.6 eV). N<sub>2</sub> adsorption-desorption isotherms were measured by a BELSORP-max (MicrotracBEL). The specific surface areas and pore size distribution were calculated based on the Brunauer-Emmett-Teller (BET) method and the nonlocal density functional theory (NLDFT) method.

### 2.6 Electrochemical Measurements.

The electrochemical measurements were carried out with an Autolab 302N potentiostat / galvanostat with a standard three-electrode system at room temperature. In the system, a graphite rod, an Ag/AgCl electrode (in saturated KCl solution) and a glassy carbon RDE (Pine Research Instrumentation) coated with catalyst films served as counter electrode, reference electrode and working electrode, respectively. To prepare the ink, 5 mg catalyst was dispersed in 1 mL of a mixture of Nafion (5 wt%, 40 μL), isopropanol (730 μL) and ultrapure water (Milli-Q Advantage A10, 230 μL). 15 μL of this ink was transferred to the surface of glassy carbon. The loading

of catalyst is  $0.38\text{ mg cm}^{-2}$ . Before linear sweep voltammetry (LSV), all electrodes were activated via cyclic voltammetry (CV) using various scan rates ( $100\text{ mV s}^{-1}$ ,  $50\text{ mV s}^{-1}$  and  $10\text{ mV s}^{-1}$ ).

### 3. RESULTS AND DISCUSSION

Firstly, the microscopic morphology of the catalyst was investigated by transmission electron microscopy (TEM). As shown in Fig. 1, the catalyst particles showed polygonal structure and uneven internal light and dark distribution. Among them, the part of black particles, which are Co nanoparticles formed during the high temperature treatment. Compared with 0.10Co-N-C (Co nanoparticle size about 10 nm), the number of Co nanoparticles in the 0.15Co-N-C catalyst is significantly increased and the size is relatively large (about 20 nm). Subsequently,  $\text{SiO}_2$  was introduced on the ZIF precursor to prevent the loss of active elements during high-temperature treatment. The metal particles in 0.10CoSi-N-C and 0.15CoSi-N-C could not be observed in the TEM images after the introduction of  $\text{SiO}_2$  shell, indicating that  $\text{SiO}_2$  protection can effectively inhibit the agglomeration of metal Co particles during the high-temperature pyrolysis process.

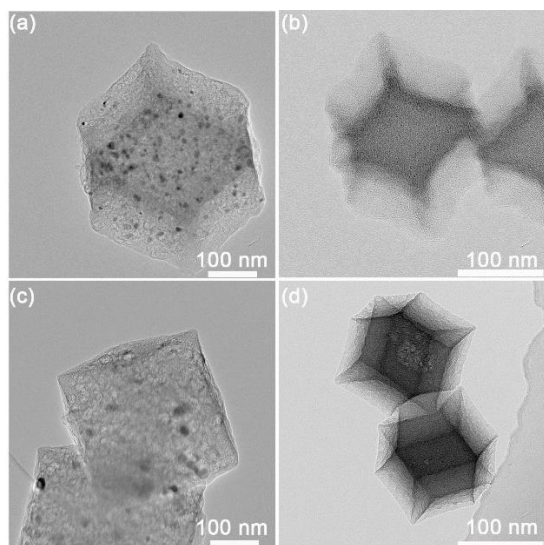


**Fig. 1.** TEM images of (a) 0.15Co-N-C, (b) 0.15CoSi-N-C and (c) 0.10Co-N-C, (d) 0.10CoSi-N-C catalyst.

In the XRD patterns (Fig. 2), the peaks at around  $26^\circ$  can be attributed to C (002). At  $44.3^\circ$  and  $51.7^\circ$ , two diffraction peaks of Co nanoparticles can be distinguished obviously, indexed to the (111) and (200) lattice planes of face-centered cubic (fcc) Co (JCPDF No. 15-0806), respectively. [4] This indicates that the four catalysts synthesized by different preparation methods are composed of amorphous C and Co nanoparticles. For

both 0.10Co-N-C and 0.15Co-N-C, the half-peak width (FWHM) of the Co(111) peak becomes larger with the protection of  $\text{SiO}_2$  shell during pyrolysis, indicating that the particle size of Co nanoparticles in 0.10CoSi-N-C and 0.15CoSi-N-C can be significantly reduced, indicating that the  $\text{SiO}_2$  coating can prevent the agglomeration of metal particles in high-temperature treatment and form highly dispersed active site. This is consistent with the results observed by TEM.

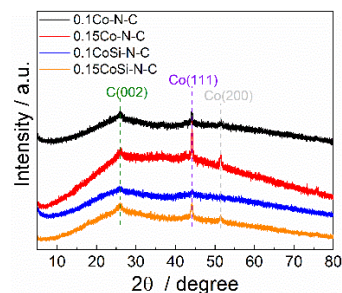


**Fig. 2.** XRD patterns of different catalyst samples.

In order to analyze the chemical structure and relative amount of the target active sites, X-ray photoelectron spectroscopy (XPS) is performed for the four catalysts. As shown in Fig. 3, the high-resolution XPS spectra of N 1s can be deconvoluted into four peaks at 398.6, 399.2, 400.9, 401.6 and 403.8 eV corresponding to pyridinic N, Co-N, pyrrolic N, graphitic N and oxidized N, respectively.[5] The form of N present in the catalyst under the protection of the  $\text{SiO}_2$  shell is converted from the oxidized state to the reduced state. The proportion of pyridine-N and Co-N is significantly increased in the 0.10CoSi-N-C and 0.15CoSi-N-C catalyst, which is always considered as the active components with electron-feeding ability for the oxygen reduction reaction.

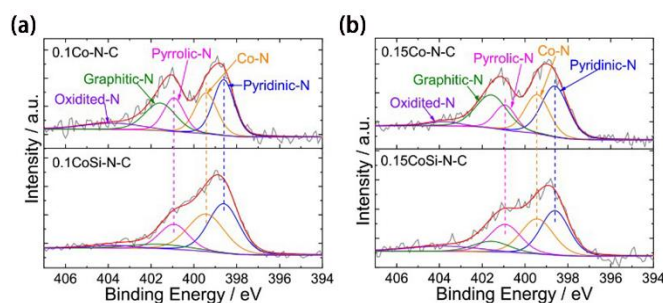


**Fig. 3.** High resolution XPS spectra of N 1s for (a) 0.10Co-N-C and 0.10CoSi-N-C and (b) 0.15Co-N-C and 0.15CoSi-N-C.

To quantitatively analyze the specific surface area of the catalysts, the nitrogen adsorption-desorption

isotherm was obtained. As shown in Fig. 4a, all four catalysts demonstrate obvious mesoporous hysteresis loop, indicating the abundant mesopores in the obtained Co-based catalyst. The pore size distribution curves of different catalysts are further obtained from nitrogen absorption-desorption isotherm via a nonlocal density functional theory (NLDFT) method (Figure 3(b)). All catalysts have gradient pore structures with micro-, meso- and macro-pores. Both Zn/Co ratio and SiO<sub>2</sub> shell will influence the porous structure in the final catalyst. As for micropore region (< 2 nm), the Zn/Co ratio is the primary factor. Abundant Zn element will increase the percentage of micropores in the catalyst, via the vaporization of metal Zn at 950 °C. By contrast, the effect of SiO<sub>2</sub> shell on the pore structure is mainly reflected in the percentage of meso- and macro-pores. This may be related to the agglomeration of Co elements and the rearrangement of carbon during the pyrolysis process. For different Zn/Co ratio, the influence of SiO<sub>2</sub> is different. As shown in Fig. 4b, the SiO<sub>2</sub> shell can reduce the volume of meso- and macro-pores for the low Co content catalyst (0.10CoSi-N-C), due to the greater inhibition of the migration and agglomeration of Co and C atoms. However, for 0.15CoSi-N-C, the SiO<sub>2</sub> shell can obviously inhibit the agglomeration of Co atoms into large particles and the collapse of the mesoporous structure. Therefore, the highly dispersed Co-based catalyst with abundant meso- and macro-pores can be obtained. As is well known, the active sites always distribute in the micropores of NPM catalysts. But, the meso- and macro-pores are also important for the mass transfer process of reactants and products [6], requiring the optimized micro-/meso-pores ratio of the catalyst to promote the catalytic activity and mass transfer process.

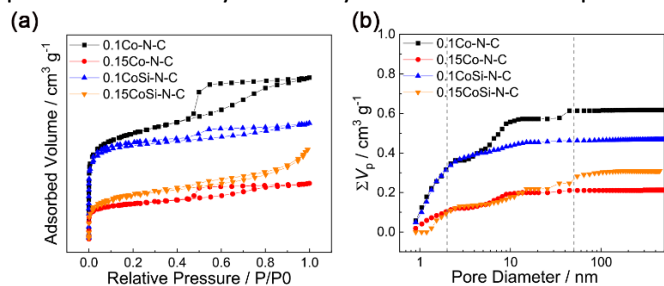


**Fig. 4.** (a) Nitrogen absorption-desorption isotherm curves, (b) Cumulative pore volume change curve

To investigate the structure-performance relationship, the ORR performance of different catalysts

was evaluated in an oxygen-saturated 0.1 M KOH solution by an RDE device. As shown in Fig. 5, 0.10Co-N-C outperformed 0.10CoSi-N-C with a half-wave potential of 0.89 V vs RHE, which is better than most of the current NPM catalysts (Table 1). Although both 0.10CoSi-N-C and 0.10Co-N-C have almost same volume of micropores, the 0.10Co-N-C exhibits much higher ORR performance, may due to the absence of mesopores (serves as the mass-transfer channel). On the other hand, compared to 0.15Co-N-C, 0.15CoSi-N-C exhibits the higher ORR performance with a half-wave potential of 0.86 V vs RHE, which is close to that of 0.10Co-N-C. It is worth mentioning that, 0.15CoSi-N-C exhibits much higher current density, even compared with 0.10Co-N-C. The volume of micro-pores is an important, but not the only parameter affecting the ORR performance. The 0.15CoSi-N-C with very small micro-pore volume exhibits good ORR performance, indicating the reasonable adjustment by Zn/Co ratio and SiO<sub>2</sub> shell can increase Co content of NPM catalyst with smaller particle size and high ORR performance.

The relationship between structure and performance can be divided into two aspect, active site (for kinetic activity) and porous structure (for mass transport). As for the active sites, the SiO<sub>2</sub> shell can regulate the chemical states of Co and N elements. Under the protection of SiO<sub>2</sub>, the form of N mostly exists in the form of pyridinic-N and Co-N, as the active centers for ORR, which is the basic requirement for higher kinetic activity. However, the porous structure is very important for the mass transfer process during the reaction. Since the active sites are distributed on the surface of pores, the diffusion rate of reactant and product will directly determine the whole catalytic activity. By carefully adjustment of Zn/Co ratio and SiO<sub>2</sub> shell, the excessive agglomeration of Co atoms and destruction of porous structure were inhibited, leading to a significant increase of active site with abundant meso- and macro-pores.

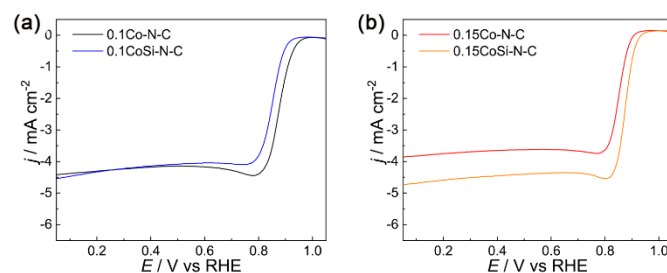


**Fig. 5.** LSV curve of (e) 0.10Co-N-C and 0.10CoSi-N-C, (f) 0.15Co-N-C and 0.15CoSi-N-C.

**Table. 1.** Comparison of ORR performance of Co-N-C catalysts under alkaline conditions

catalysts	Mass Loading (mg cm <sup>-2</sup> )	Half-wave potential (V vs. RHE)	References
0.15CoSi-N-C	0.38	0.86	This work
C-SAs@NC	0.611	0.82	[7]
Coll-A-rG-O	0.6	0.81	[8]
CoP-CMP800	0.6	0.81	[9]
Co-N-C-NS	0.464	0.84	[10]
ZIF-CB-700	0.382	0.814	[11]
0.15Co-N-CB	0.382	0.87	[12]

#### 4. CONCLUSION

In this work, the ORR performance of ZIF-derived catalysts with different active site density and pore structures were fabricated by adjusting Zn/Co ratio and SiO<sub>2</sub> shell. The experimental results show that SiO<sub>2</sub> coating can effectively prevent the agglomeration of Co nanoparticles during high-temperature carbonization and induce the structural transformation of N, resulting in a significant increase in the percentage of active components (pyridinic-N and Co-N) in the catalysts. As for the porous structure, Zn/Co ratio and SiO<sub>2</sub> shell will have the particular influence on the micro-pore and meso-/macro-pores, respectively. For ZIF precursors with low Co element content, the protective effect of SiO<sub>2</sub> will inhibit the migration of Co atoms and significantly reduce the number of mesopores. For the ZIF precursors with high Co element content, SiO<sub>2</sub> shell can reduce the excessive agglomeration of Co atoms and protect the meso-pore in the catalyst, which is beneficial to increase the active site density (high Co content) and mass-transfer efficiency (abundant meso-/macro-pores). This work can provide an insight for high metal content ORR catalyst design, to increase the active site density and reduce the thickness of catalyst layer in alkaline fuel cells and has certain guiding significance for the design of

non-precious metal ORR catalysts for the subsequent alkaline fuel cell cathodes.

#### ACKNOWLEDGEMENT

This research is supported by National Natural Science Foundation of China (22005214 and 21875161).

#### REFERENCE

- [1] Zhu C, Li H, Fu S, Du D, Lin Y. Highly Efficient Nonprecious Metal Catalysts towards Oxygen Reduction Reaction Based on Three-Dimensional Porous Carbon Nanostructures. *Chem Soc Rev*, 2016, 45: 517-531.
- [2] Jiao Y, Zheng Y, Jaroniec M, Qiao S Z. Design of Electrocatalysts for Oxygen- and Hydrogen-Involving Energy Conversion Reactions. *Chem Soc Rev*, 2015, 44: 2060-2086.
- [3] Shang L, Yu H, Huang X, et al. Well-Dispersed ZIF-Derived Co,N-doped Carbon Nanoframes through Mesoporous-Silica-Protected Calcination as Efficient Oxygen Reduction Electrocatalysts. *Adv Mater*, 2016, 28: 1668-1674.
- [4] Liu C, Wang J, Li J, et al. Electrospun ZIF-based Hierarchical Carbon Fiber as an Efficient Electrocatalyst for the Oxygen Reduction Reaction. *J Mater Chem A*, 2017, 5: 1211-1220.
- [5] Wang X X, Cullen D A, Pan Y T, et al. Nitrogen-Coordinated Single Cobalt Atom Catalysts for Oxygen Reduction in Proton Exchange Membrane Fuel Cells. *Adv Mater*, 2018, 30.
- [6] Shang L, Yu H, Huang X, et al. Well-Dispersed ZIF-Derived Co,N-doped Carbon Nanoframes through Mesoporous-Silica-Protected Calcination as Efficient Oxygen Reduction Electrocatalysts. *Adv Mater*, 2016, 28: 1668-1674.
- [7] Han X, Ling X, Wang Y, et al. Generation of Nanoparticle, Atomic-Cluster, and Single-Atom Cobalt Catalysts from Zeolitic Imidazole Frameworks by Spatial Isolation and Their Use in Zinc-Air Batteries. *Angew Chem Int Ed Engl*, 2019, 58: 5359-5364.
- [8] Han J, Sa Y J, Shim Y, et al. Coordination Chemistry of [Co(acac)<sub>2</sub>] with N-Doped Graphene: Implications for Oxygen Reduction Reaction Reactivity of Organometallic Co-O<sub>4</sub>-N Species. *Angew Chem Int Ed Engl*, 2015, 54: 12622-12626.
- [9] Wu Z S, Chen L, Liu J, et al. High-Performance Electrocatalysts for Oxygen Reduction Derived from Cobalt Porphyrin-Based Conjugated Mesoporous Polymers. *Adv Mater*, 2014, 26: 1450-1455.
- [10] Lee J H, Park M J, Yoo S J, et al. A Highly Active and Durable Co-N-C Electrocatalyst Synthesized Using

Exfoliated Graphitic Carbon Nitride Nanosheets. *Nanoscale*, 2015, 7: 10334-10339.

[11] Zhang J, Zhu W, Pei Y, et al. Hierarchically Porous Co-N-C Cathode Catalyst Layers for Anion Exchange Membrane Fuel Cells. *ChemSusChem*, 2019, 12: 4165-4169.

[12] Zhu W, Pei Y, Liu Y, et al. Mass Transfer in a Co/N/C Catalyst Layer for the Anion Exchange Membrane Fuel Cell. *ACS Appl Mater Interfaces*, 2020, 12: 32842-32850.